Novel insights into old anticancer drugs

Zanden, S.Y. van der

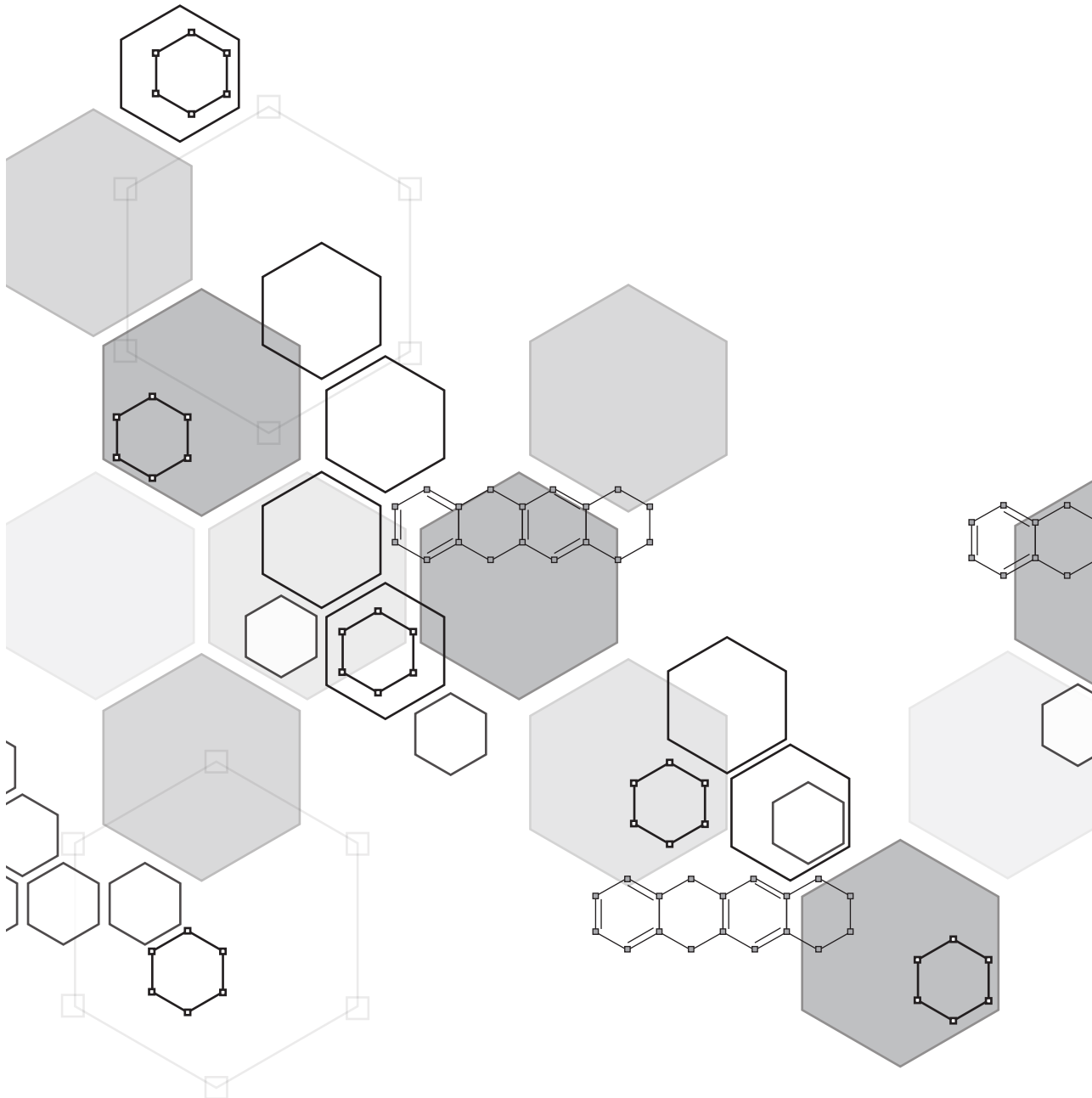

Nuclear DNA sensors re-localize upon chromatin damage; do they play a role in anthracycline induced cell death?

7

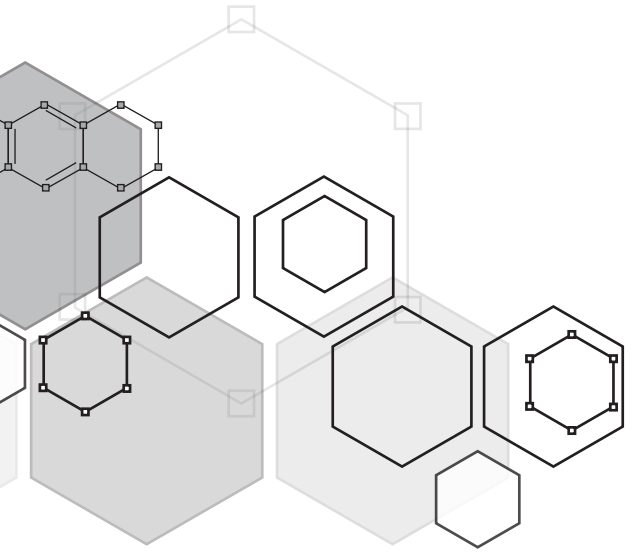

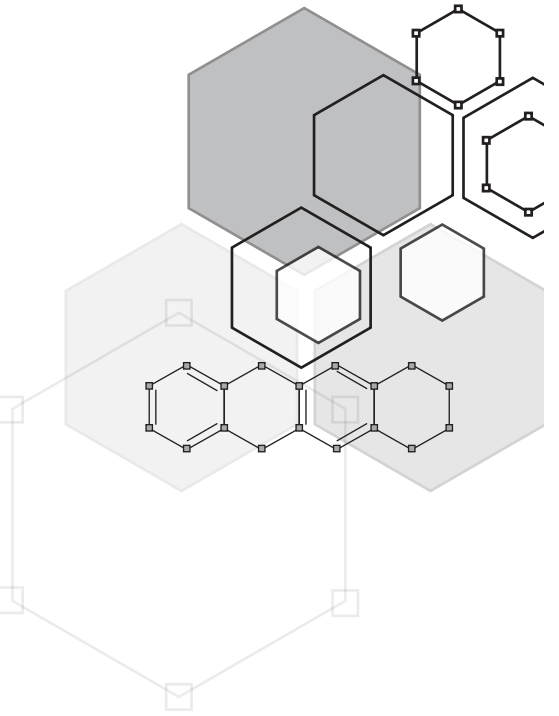

Sabina Y. van der Zanden, Feija L. Hamoen, Jimmy J. Akkermans, Noa Linthorst, Daniel Borràs, Lennert Janssen, George M.C. Janssen, Peter A. van Veelen, Jacques Neefjes

Manuscript in preparation

ABSTRACT
Since the 1970s the anthracycline drugs daunorubicin and doxorubicin are extensively used as single drugs or in combination therapies to treat many types of tumors. Even after 50 years of clinical usage, the exact molecular mechanism by which these drugs function is still not fully known. A well accepted mechanism of action is the formation of DNA damage, via interference with the catalytic cycle of topoisomerase II. However, a recently discovered second mechanism – chromatin damage as the result of histone eviction – was shown to be the main cytotoxic mechanism of these drugs. How histone eviction subsequently leads to the induction of cell death is poorly understood. Here, we identified three nuclear DNA sensors (IFI16, IFIX and MNDA) active in the innate immune response to DNA viruses that specifically re-localize to DNA upon histone eviction, and novel interaction partners for these sensors that might play a role in anthracycline-induced cytotoxicity.

INTRODUCTION
The anthracycline drugs doxorubicin (Doxo) and its analogs epirubicin (Epi) and daunorubicin (Dauno) are cornerstones in the treatment of different types of hematological and solid tumors for half a century [1, 2]. A well accepted mechanism of action for these chemotherapeutic drugs is the induction of DNA double strand breaks, by blocking the catalytic cycle of the enzyme topoisomerase IIα (Topo IIα) and thereby forming topoisomerase-DNA adducts [3, 4]. Recently, we and others described that anthracyclines such as Doxo can also induce chromatin damage by eviction of histones. However, how histone eviction then leads to the initiation of cell death remains unclear [5, 6]. The occurrence of large stretches of histone free DNA, as is the case for cells treated with anthracycline drugs, is an unusual situation in eukaryotic cells, where the DNA is usually tightly packed in nucleosomes. The formation of nucleosomes ensures that the long DNA molecules can be condensed to fit into the nucleus, but also controls (tissue-specific) gene expression [7]. We hypothesized that the histone free DNA induced by these anthracycline drugs can be recognized by specific proteins to mask the naked DNA or to initiate a stress response. Potential protein candidates to fulfill this function are the DNA sensing proteins of the PYHIN protein family. This protein family consist of four proteins (PYHIN 1-3 and AIM2), of which three are expressed in the nucleus [8]. All four proteins consist of an N-terminal pyrin (PYD) domain, a death domain DD protein fold that can form homotypic interactions with other PYD-containing proteins. In general, these DD domain protein interactions result in the formation of complexes which are known to play a role in inflammation, cell cycle and apoptosis [9]. In addition to the PYD domain, these DNA sensors consist of one or two DNA binding HIN200 domains. The best studied nuclear DNA sensor of this protein family, PYHIN 2 (also known as IFI16 or interferon inducible protein 16), is described to play a role in the detection and response to double stranded DNA viruses, such as HCMV, KSHV and HIV [10-12]. We wondered whether the histone-free DNA generated by anthracyclines could be sensed by the nuclear DNA sensing proteins PYHIN 1 (IFIX), IFI16 and/or PYHIN 3 (MNDA) thereby connecting the innate immune response to anthracycline induced cell death (Figure 1A).

RESULTS
Histone eviction dependent re-localization of nuclear DNA sensors
To determine whether nuclear DNA sensors play a role in anthracycline induced cell death, we evaluated the localization of three of these DNA sensors (PYHIN1-3, or

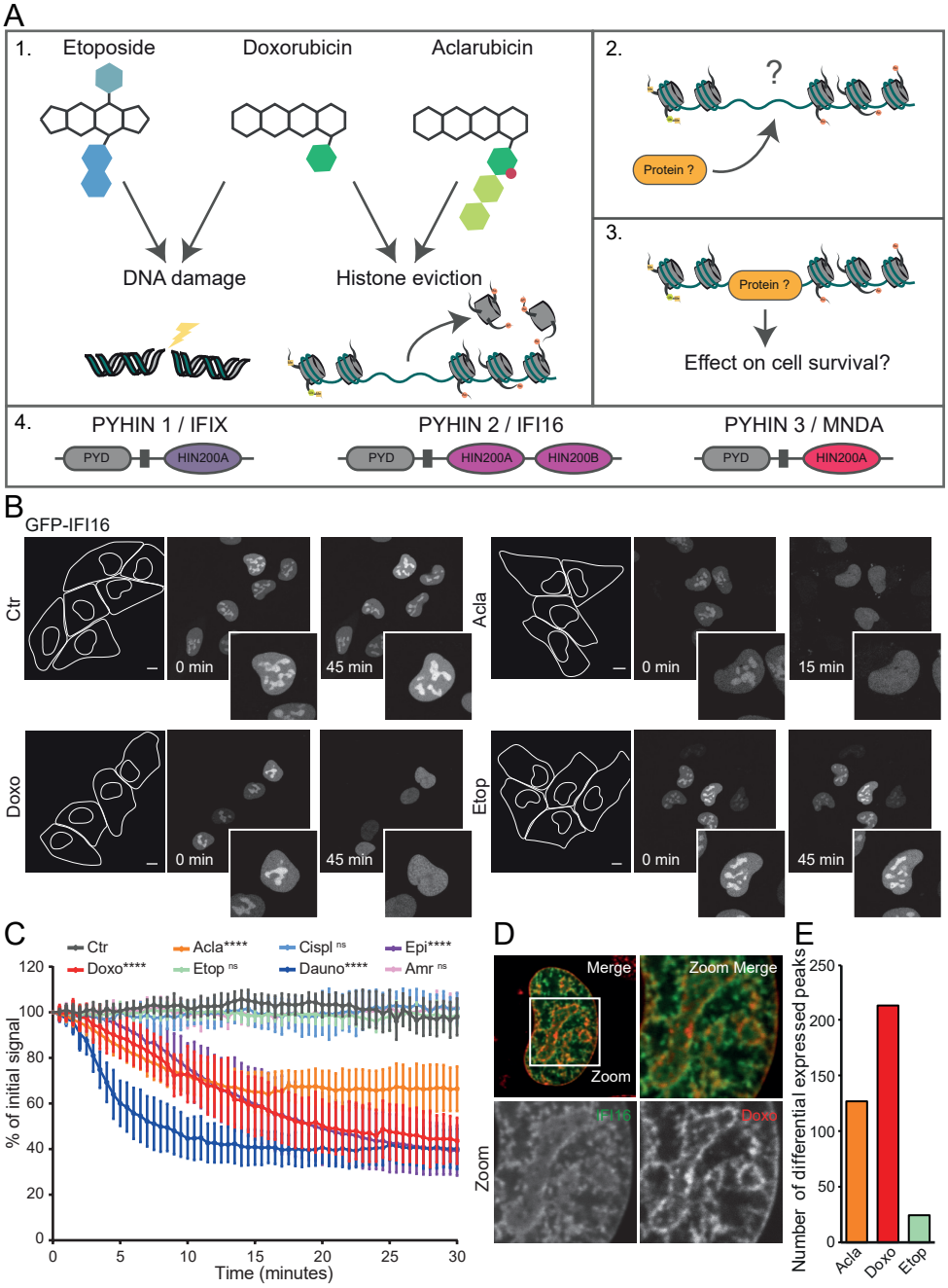

Figure 1. Nuclear DNA sensors re-localize upon histone eviction. *(A) Schematic representation of anthracycline mechanism of action: 1. Anthracycline drugs can induce DNA damage via the formation of topoisomerase IIα-DNA adducts and/or evict histones following intercalation into the DNA resulting in chromatin damage. 2. What happens after histones are evicted? 3. Are there proteins that detect the anthracycline induced 'naked DNA' and do*

Figure 1. Continued (A). *they play a role in anthracycline induced cytotoxicity? 4. Schematic domain organization of three nuclear DNA sensing proteins of the PYHIN protein family. (B) MelJuSo cells transiently expressing GFP-tagged IFI16 are followed by time-lapse confocal microscopy upon treatment with various drugs: Doxo 10μM, Acla 5μM, Etop 10μM. Scale bar, 10 μm. (C) Quantification of the fluorescent intensity in the nucleoli of cells in B. Ordinary Two-way ANOVA with Turkey's multiple comparison test; ns, not significant; ****P < 0,0001. (D) Localization of GFP-tagged IFI16 in MelJuSo cell nucleus treated with Doxo 10μM for 30 minutes. (E) Number of differential expressed reads for endogenous IFI16-ChIP sequencing in MelJuSo cells, upon treatment for 2 hour with the different drugs. Acla 10μM, Doxo 10μM and Etop 10μM.*

IFIX, IFI16 and MNDA respectively) before and after treatment with different anticancer drugs. GFP-tagged IFIX, IFI16 or MNDA were transiently expressed in MelJuSo cells, allowing detection of the fluorescent signal over time upon treatment with different genotoxic stimuli (Figure 1B, 1C and Figure S1-S3). At steady state, the DNA sensors localized in the nuclear where it accumulated in the nucleoli. Upon treatment with histone evicting anthracycline drugs (Doxo, Acla, Epi or Dauno), the DNA sensors rapidly re-localized from the nucleoli to the nucleosol. This re-localization was specific for chromatin damage, since drugs unable to induce histone eviction (Etop, cisplatin; Cispl and amrubicin; Amr) did not change DNA sensor localization upon treatment. To identify whether the DNA sensors were able to detect the histone free DNA upon eviction of histones, we had a closer look at the location of IFI16 upon treatment with Doxo. Thirty minutes post Doxo treatment, IFI16 localization partially overlapped with the Doxo (which is fluorescent) intercalated into the DNA (Figure 1D), indicating that IFI16 indeed sensed the Doxo-induced histone-free DNA. To validate this observation, we immunoprecipitated endogenous IFI16 upon treatment of MelJuSo cells with Doxo, Acla and Etop, and analyzed DNA binding by sequencing (ChIP-seq). Indeed, treatment with histone evicting drugs increased the number of differentially expressed peaks, indicating that histone eviction induces DNA binding of IFI16 (Figure 1E).

Identification of novel interacting proteins

Upon histone eviction, the nuclear DNA sensors IFIX, IFI16 and MNDA re-localize from the nucleoli to the nucleosol, potentially to detect the histone free DNA regions. However, what happens after these DNA sensors bind the DNA is unclear. In the context of HSV-1 viral infection, IFI16 reduces viral replication via repression of viral gene expression [13]. This suggests that the DNA sensors could affect the transcriptome while binding the DNA following histone eviction induced by the anthracycline drugs (Figure 2A). Alternatively, upon DNA binding they initiate the formation of protein complexes via their PYD-domain, which are known to play a role in the formation and activation of the inflammasome [9]. However, the molecular mechanism for the latter is unknown. To identify novel interactors for the DNA sensors, we performed a Bio-ID proximity labeling assay. BirA-tagged DNA sensors were transiently overexpressed and upon lysis, biotinylated proteins were precipitated and analyzed by mass spectrometry (Figure 2A and Table 1). Novel interactions, which were selected based on their known role in cell death and innate immunity pathways, with the deubiquitinating enzyme USP7, the E3-ligase TRIM26 and the ATP-dependent DNA helicase XRCC6 were validated by co-immunoprecipitation experiments (Figure 2B-D). IFIX preferentially interacted with TRIM26 and XRCC6 while IFI16 and MNDA preferred interactions with USP7. This suggests that the DNA sensors have some specificity in recruiting ligands to the DNA. Interestingly, upon treatment with Doxo,

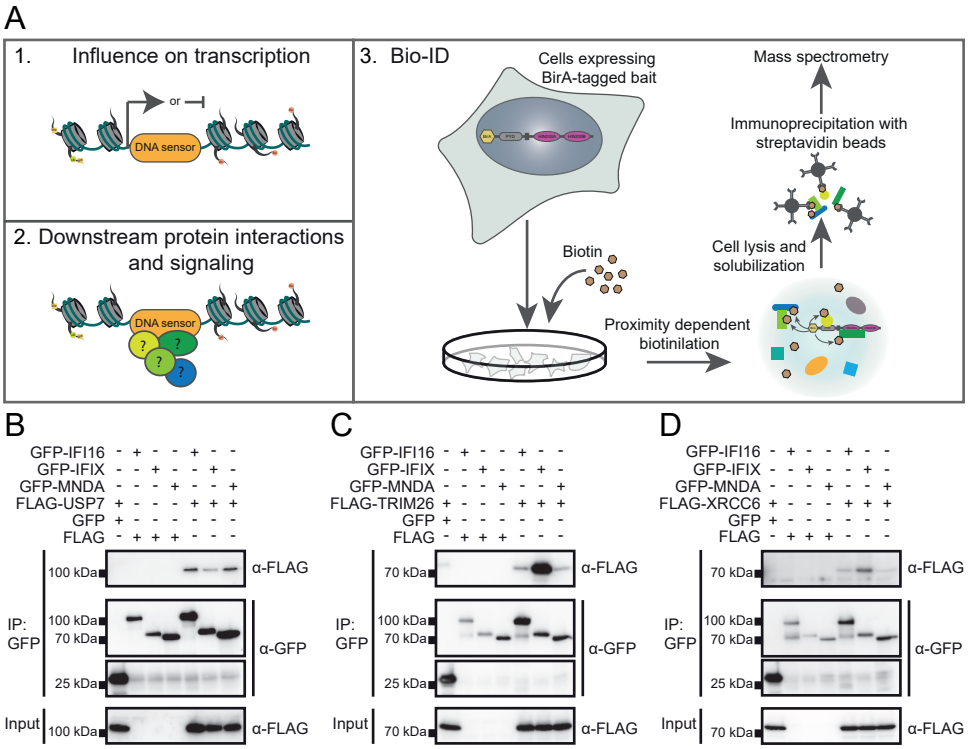

Figure 2. Identification of nuclear DNA sensor-interacting proteins. *(A) Schematic representation potential consequences of histone eviction. 1. Binding of nuclear DNA sensor to the anthracycline induced histone free DNA might induce or repress transcription. 2. After binding of the histone free DNA the DNA sensor recruit, bind and activate other proteins to initiate downstream signaling. 3. Overview of Bio-ID workflow for DNA sensors interacting protein identification. BirA tagged DNA sensors are transiently expressed in HEK293T cells, upon incubation with biotin protein in close proximity of the bait are biotinylated. Upon lysis, biotinylated proteins were isolated and identified by mass spectrometry. (B – D) Validation of some of the interactions found by Bio-ID: USP7 (B), TRIM26 (C) and XRCC6 (D) with the nuclear DNA sensors.*

transiently expressed mTurq-USP7 re-localized in a way similar to the DNA sensors (Figure S4).

Domain characterization of USP7 and TRIM26

To identify the responsible interacting domain for the hits determined by Bio-ID, we cloned different truncation mutants of USP7 and TRIM26 (Figure 3A and 3C). Subsequently, HEK293T cells were transiently transfected with GFP-IFI16 and the various FLAG-tagged USP7 constructs and interaction were assessed by co-immunoprecipitation. Both full length USP7 and USP7-NTD-CAT interacted with IFI16, indicating that the catalytic domain of USP7 count mediate this interaction (Figure 3B).
To identify which domain of TRIM26 interacts with the DNA sensors, its different domains were immunoprecipitated with IFIX, the strongest interactor according to the Bio-ID and co-immunoprecipitation validation. HEK293T cells were transiently transfected with GFP-IFIX and the different FLAG-TRIM26 constructs (Figure 3C). IFIX

		Exclusive Unique Peptide Count						
Protein ID	MW	GFP-BirA	GFP-BirA-IFI16	Coverage	GFP-BirA-IFIX	Coverage	GFP-BirA-MNDA	Coverage
IFI16	88 kDa	0	99	77%	6	16%		
IFIX	55 kDa	0			49	74%		
MNDA	46 kDa	0					43	78%
DYNC1H1	532 kDa	2	56	18%	67	20%	39	11%
IPO7	120 kDa	8	25	30%				
HUWE1	482 kDa	5	24	9%	30	10%	14	5%
USP7	128 kDa	2	17	22%	9	12%	7	9%
GTF2F2	28 kDa	0	10	33%				
PPM1G	59 kDa	2	7	14%				
ARID3B	61 kDa	2	7	18%				
XRCC6	70 kDa	3	7	8%	11	25%	13	28%
NACC1	57 kDa	0	6	20%				
ZBTB10	95 kDa	0	6	11%				
DDX21	87 kDa	0	5	10%	7	11%	11	18%
WDR70	73 kDa	0	5	9%	6	11%		
CLTC	192 kDa	7			29	24%		
PARP1	113 kDa	13			20	27%	28	36%
EIF3A	167 kDa	4			20	17%	14	11%
MYBBP1A	149 kDa	5			15	15%	27	26%
MSH6	153 kDa	6			14	12%		
PPM1G	59 kDa	2			12	22%		
TRIM26	62 kDa	0			10	24%		
DNMT1	183 kDa	3			10	8%	12	9%
MYH10	229 kDa	2			9	10%		
IQGAP1	189 kDa	2			9	9%		
ESF1	99 kDa	0			8	11%		
MSH2	105 kDa	2			7	10%	6	7%
TPX2	86 kDa	0			7	11%	16	26%
NACC1	57 kDa	0			7	22%		
SMC1A	143 kDa	0			7	6%		
GTF2F2	28 kDa	0			6	22%	10	36%
POLA1	166 kDa	0			6	6%		
ZBTB10	95 kDa	0			4	6%	5	8%
DDX10	101 kDa	0					12	15%
SERPINB3	45 kDa	0					11	33%
NOP14	89 kDa	0					7	10%

Table 1. *Selection of potential nuclear DNA sensor interacting proteins identified by Bio-ID.*

co-immunoprecipitated full length TRIM26, TRIM26-ΔRING, TRIM26-ΔRINGΔBox and TRIM26-PRYSPRY, suggesting that the interaction with IFIX is mediated by the PRYSPRY domain of TRIM26 (Figure 3D). Little is known about TRIM26 interacting proteins, but the interaction described with TBK1, which plays a role in TBK1 activation upon RNA viral infection, is also mediated by this PRYSPRY domain [14].

Ubiquitination of nuclear DNA sensors

Since the CAT domain could be responsible for the de-ubiquitinating activity of USP7, we wondered whether IFI16 can be ubiquitinated. To test this, GFP-IFI16 and HA-Ub were overexpressed in Hela cells. Indeed, ubiquitinated IFI16 was de-

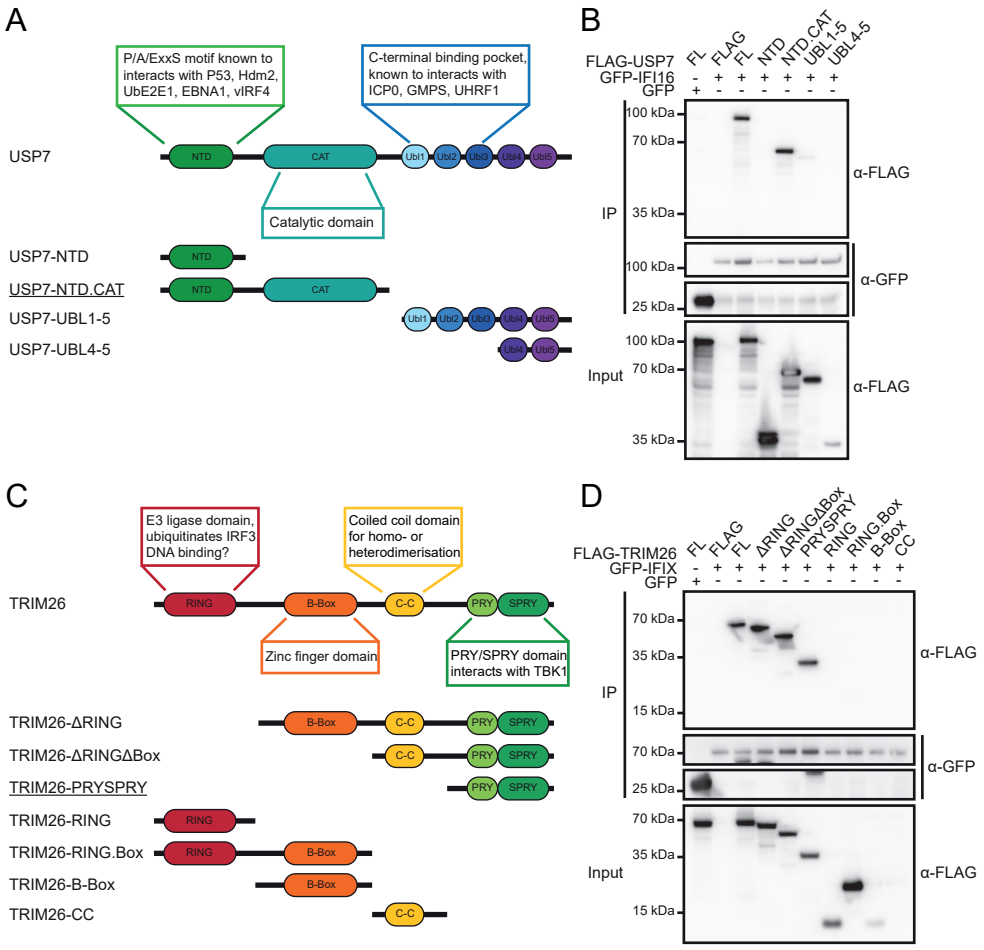

Figure 3. Domain characterization of USP7 and TRIM26. *(A) Schematic domain organization of USP7. (B) Interactions between IFI16 and USP7 domains assayed by co-immunoprecipitation. (C) Schematic domain organization of TRIM26. (D) Interactions between IFIX and TRIM26 domains assayed by co-immunoprecipitation.*

tectable and treatment with Acla slightly increased the amount of IFI16 ubiquitination (Figure 4A). Possibly USP7 could de-ubiquitinate IFI16 and hereby influence its function. Therefore we generated the USP7C223S catalytic mutant, which renders the enzyme catalytically inactive, and assessed its interacting and de-ubiquitination activity towards the DNA sensors compared to wild-type USP7. While the interaction with IFI16 did not change compared to wild-type USP7 (Figure 4B), USP7 partially reduced ubiquitination of the DNA sensors IFI16 (Figure 4C) and MNDA (Figure 4D), but not for IFIX (Figure 4E). Only for MNDA ubiquitination is depended on the catalytic activity of USP7, suggesting MNDA could be a potential substrate for USP7. Since the E3-ligase TRIM26 also interacted with the different DNA sensors, we wondered whether TRIM26 affects their ubiquitination status. Indeed, TRIM26 was found to increase poly-ubiquitination of MNDA whereas IFI16 remained unaffected. While

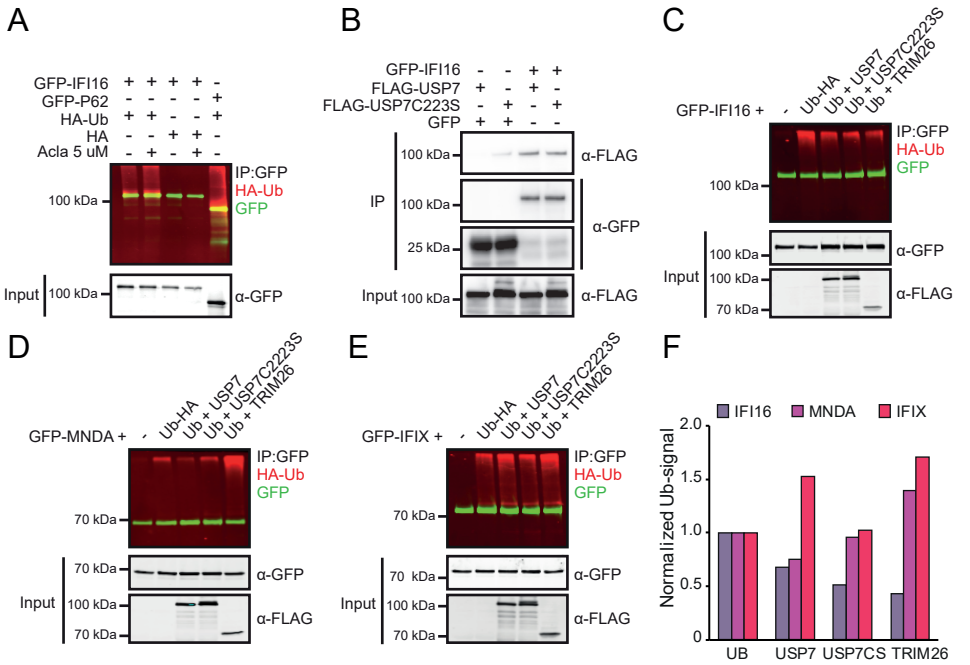

Figure 4. Ubiquitination of nuclear DNA sensors. *(A) Ubiquitination status of IFI16 expressed in Hela cells. GFP-P62 was expressed as positive control. Ubiquitination status of GFP-substrate (green) was assessed by immunoblots against HA (red). (B) Interaction between wild-type and catalytic death USP7 (USP7C233S) mutant and IFI16. (C - E) Ubiquitination status of IFI16 (C), MNDA (D) and IFIX (E) as a function of catalytic activities of USP7, USP7C223S and TRIM26 co-expressed with HA-Ub in HEK293T cells. (F) Quantification of (C – E), normalized ubiquitin signal of the three nuclear DNA sensor.*

IFIX interact with TRIM26 most efficiently, it was only poorly ubiquitinated (Figure 4C-E). Together, these data suggest that MNDA might be subjected to TRIM26/USP7 controlled ubiquitination unlike its family members IFI16 and IFIX. These two DNA sensors may recruit the ubiquitin machinery for the manipulation of other substrates and/or pathways that are –as yet- unclear.

Interferon stimulation affects anthracycline sensitivity

Re-localization of the DNA sensors upon histone eviction suggest a role in anthracycline-induced cell death. Interestingly, many tumor cells do not express these DNA sensors. IFI16 for example is mainly expressed in cells of the immune system, as well as fibroblasts, epithelial-, and endothelial cells, and altered expression has been shown to play a role in tumor development [15-17]. However, both type I (α and β) and type II (γ) interferons positively regulate the expression of the PYHIN-family of proteins [18]. Therefore, we decided to investigate whether stimulation with interferons would upregulate the expression of IFI16 in MelJuSo cells, and if this could affect their cell survival upon treatment with the anthracycline drugs. To determine IFI16 expression following stimulation with type I (IFNβ) and type II (IFNγ) interferons, we stimulated MelJuSo cells for 8, 24 and 48 hours and visualized protein expression by Western blot (Figure 5A and B). As expected, IFI16 protein levels

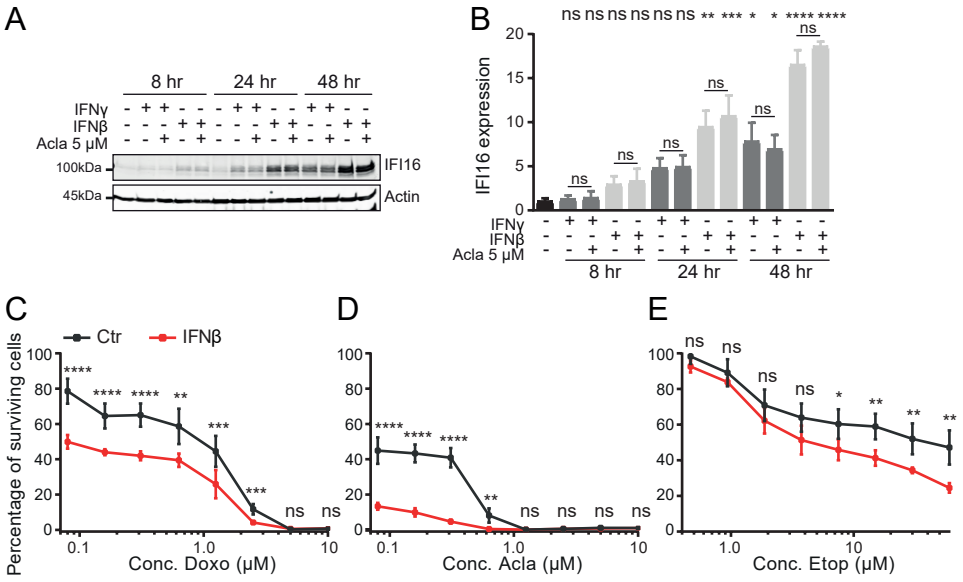

Figure 5. Interferon stimulation upregulates IFI16 expression and sensitizes cells to anticancer drugs. *(A) IFI16 protein expression upon stimulation with interferon. MelJuSo cells are stimulated with IFNγ or IFNβ (100ng/ml) for the indicated time points. One hour prior to collection, indicated samples were treated with Acla 5 μM. (B) Quantification of A. Ordinary One-way ANOVA with Turkey's multiple comparison test; ns, not significant; *P < 0.05; **P < 0.01; ***P < 0.001; ****P < 0,0001. (C - E) Cell Titer blue viability assay. MelJuSo cells with or without IFNβ stimulation (24 hours prior to treatment) were treated with various concentration of Doxo (C), Acla (D) and Etop (E). Multiple unpaired t- test; ns, not significant; *P < 0.05; **P < 0.01; ***P < 0.001; ****P < 0,0001.*

strongly increased over time by both IFNβ and IFNγ stimulation. Of note, treatment with the histone evicting drug Acla did not affect IFI16 expression levels (Figure 5A and B). To determine the role of elevated IFI16 expression levels on sensitivity towards histone evicting drugs, we determined the cytotoxicity of Doxo, Acla or Etop in MelJuSo cells either pre-stimulated or not with IFNβ. Interferon stimulation sensitized MelJuSo cells especially for Acla (histone eviction only) and Doxo (histone eviction and DNA damage) treatment and had only marginal effects on Etop (DNA damage only) (Figure 5C-E). These data form preliminary evidence that IFI16 might play a role in detection of histone free DNA induced by the anthracycline drugs, and subsequent initiation of cell death.

CONCLUSION AND FUTURE DIRECTIONS

Every year over one million patients with different types of cancer receive anthracycline based-treatments. While these drugs are very effective anticancer drugs, their exact mechanism of action is disputed. Since their discovery decades ago, various working mechanism have been suggested. These include; interfering with the catalytic cycle of Topo IIα resulting in the induction of DNA double strand breaks, the formation of free radicals, and induction of chromatin damage via eviction of histones [4-6, 19]. Our recent work indicated that the latter mechanism might be the most relevant activity for the anticancer mechanism of these drugs [20]. However,

how chromatin damage then leads to the initiation of cell death remains unclear. We hypothesized that histone free DNA, a consequence of histone eviction, could be sensed by nuclear proteins to either restore this unnatural situation or to initiate cell death. Here, we identify three proteins from the PYHIN protein family (IFIX, IFI16 and MNDA) that re-localized to DNA upon treatment with the anthracyclines Doxo, Acla, Epi or Dauno, but not with drugs that are unable to evict histones (Figure 1A, B and Figure S1, S2 and S3). In addition, DNA binding of IFI16 was increased by the histone eviction drugs Doxo and Acla (Figure 1E). Thus, chromatin damage as a result of anthracycline treatment results in increased DNA binding of DNA sensors, potentially signaling to the cell that undesired naked DNA is present.

But what happens after these DNA sensors detect the histone free DNA? In the context of viral infection Unterholzner et. al. reported that detection by IFI16 induces IFNβ production via recruitment and activation of the STING-TBK1-IRF3 pathway [21]. Production of IFNβ, which is a hallmark for a functional innate immune response, via DNA sensing by IFI16 might also play a role in the anti-tumor response of anthracyclines in vivo. Alternatively, IFI16 is involved in transcriptional repression. Johnstone et. al. showed that IFI16 can repress transcription of a GAL4 reporter construct and the HCMV gene UL54 reporter construct via binding of its HIN200 domain [22]. In human embryo lung fibroblasts, IFI16 downregulates viral gene expression and hereby replication of HCMV by preventing the binding of the transcription factor Sp1 [23]. Similarly, IFI16 inhibits HSV-1 viral replication via repression of HSV-1 gene expression [24, 25]. Mechanistically, IFI16 alters the epigenetic state of the viral DNA [24] and likely restricts viral gene expression by inducing a viral heterochromatin (H3K9me3) state [25]. This suggests that IFI16 might repress transcription upon anthracycline-induced histone eviction. Interestingly, it is known that the anthracycline drugs effects the transcriptome [5]. Therefore, studying the role of these different nuclear DNA sensors on altered transcription of anthracycline treated cells would be an interesting next step.

Others have described that IFI16 can interact with p53 via its HIN200A domain to regulate the cell cycle and apoptosis [26]. This interaction does not impact p53 expression or stability, but rather its DNA binding capability. Co-expression of IFI16 and p53 also resulted in a dose-dependent increase of p53-mediated transcription activation of the CAT reporter. In addition, the interaction of IFI16 with p53 modulates p53 function and target gene regulation to control cell cycle regulation via p21 in U2OS cells [27]. In our Bio-ID screen we identified multiple potential interacting proteins for IFIX, IFI16 and MNDA, including the DUB USP7 and the E3-ligase TRIM26 (Table 1 and Figure 2B and C). Since both IFI16 and USP7 are known to interact with p53 [26, 28], USP7 might be recruited to de-ubiquitinate p53 and initiate a stress response upon detection of the histone free DNA by IFI16. In support of this, treatment with Doxo indeed resulted in redistribution of mTurq-tagged USP7 in a manner similar as the DNA sensors (Figure S4). Besides a role for USP7 and p53, sensing of histone free DNA might be linked to activation of the innate immune system via recruitment of TRIM26, since TRIM26 is described to interact with and activate TBK1 [14]. How DNA sensing and binding of USP7 or TRIM26 affects anthracycline induced cell death remains unclear. But p53-mediated apoptosis initiation upon complex formation of the DNA sensors with USP7 and/or TRIM26 would be of interest for further investigation.

The human PYHIN protein family was initially identified as interferon inducible genes due to their sequence similarity to the murine gene cluster [29]. Expression of these proteins is positively regulated by type I and/or type II interferons [18]. We show

that interferon stimulation of MelJuSo cells also resulted in increased expression of IFI16, which increased the sensitivity to treatment with anthracycline drugs (Figure 5). This might indicate that indeed IFI16 plays a role in histone eviction-mediated cell death in these cells, although this should be confirmed in IFI16 depleted cells. If so, our observations are supported by a study of Fujiuchi et. al. who showed that enhanced expression of IFI16 in the breast cancer cell line MCF-7 increased their susceptibility toward ionizing radiation-induced apoptosis [30]. Enhanced IFI16 expression resulted in p53-mediated apoptosis upon irradiation via the known p53 target genes p21, Hdm2 and bax. Together, this argues that IFI16 can initiate p53-mediated apoptosis upon sensing of DNA/genotoxic stress in general.
Collectively, our work suggests that the nuclear DNA sensors IFIX, IFI16 and MNDA might function as novel players in anthracycline induced cell death. We defined the interactions between the sensors with the ubiquitin machinery (USP7 and TRIM26) and a DNA helicase (XRCC6) involved in innate immunity. Further research is needed to unravel their exact molecular mechanism and contribution in anthracycline-induced chromatin damage. But this could yield new insights in the cellular response to an old anticancer drug family that employs the innate immune system.

MATERIALS AND METHODS

Reagents and antibodies

Doxorubicin, epirubicin, and cisplatin were obtained from Accord Healthcare, UK. Etoposide was obtained from Pharmachemie, the Netherlands. Daunorubicin was obtained from Sanofi-Aventis, the Netherlands. Aclarubicin (sc-200160) and amrubicin (sc-207289) were purchased from Santa Cruz Biotechnology, USA. All the drugs were dissolved according to the manufacturer's formulation, aliquoted and stored at −20°C for further use. Rabbit anti-GFP (generated in house, NKI, The Netherlands, 1:1000 [31]), HRP-Protein A (10-1023, Invitrogen, 1:5000), HRP-conjugated anti-FLAG M2 (Mouse, A8592, Sigma, 1:5000), Mouse anti-HA (16B12, Covance, 1:1000), IRDye 680LT goat anti-mouse IgG (H+L) (926-68020, Li-COR, 1:20000), IRDye 800CW goat anti-rabbit IgG (H+L) (926-32211, Li-COR, 1:10000), mouse anti-FLAG M2 (F3165, Sigma, 1:5000), mouse anti-β-actin (A5441, Sigma, 1:10000), mouse anti-IFI16 (Santa Cruz, sc-8023, 1:500).

Cell culture and constructs

MelJuSo cells were cultured in IMDM medium supplemented with 8% FCS. HEK293T and Hela cells were cultured in DMEM medium supplemented with 8% FCS. Cell lines were maintained in a humidified atmosphere of 5% CO_2 at 37°C and regularly tested for the absence of mycoplasma. IFIX amplified from IMAGE # 40033401 and MNDA amplified from IMAGE # 5223430 were cloned into the mGFP-C1 vector by BglII-Asp718I restriction sites. IFI16 was amplified from Addgene clone #35064 and cloned into the pEGFP-C2 vector by BamHI/Bsp120I restriction sites. USP7 was amplified from addgene clone # 16655 and cloned into the FLAG-C1 and mTurq-C1 vector by SalI/BamHI restriction sites. Inactive mutant of USP7 (C223S) was created by site directed mutagenesis. USP7 truncation mutant constructs (FLAG-C1 vector) were obtained by IVA cloning [32]. TRIM26 was described before and kindly gifted by JL Parsons [33], amplified and cloned into the FLAG-C1 vector by SalI/BamHI restriction sites. TRIM26 truncation mutant constructs (FLAG-C1 vector) were obtained by IVA cloning. XRCC6 was amplified from the pDONR223 library and cloned into the FLAG-C1 vector by SalI/BamHI restriction sites. BirA-GFP constructs were created

by amplification of the gene from the full length constructs (pEGPP-C2-IFI16, mGFP-C1-IFIX and mGFP-C1-MNDA) and cloned into the mGFP-BirA-C1 vector [34] using SalI/BamHI (for IFIX and IFI16) and HindIII/SalI (for MNDA) restriction enzymes. For ubiquitination assays HA-Ub pcDNA3.1, 2xHA-C1 were previously described [35]. All constructs were sequence verified.

Confocal microscopy
For live cell imaging MelJuSo cells were seeded in a 35mm glass bottom petri dish (Poly-dlysine-Coated, MatTek Corporation), transfected (effectene, Qiagen) 16 hours later and treated as indicated. Time-lapse confocal imaging was performed on a Leica SP8 confocal microscope system, 63x lens, equipped with a climate chamber. Images were quantified using Image J software.

ChIP-sequencing
A total of 5 x $10^{\wedge 7}$ MelJuSo cells were used per sample and treated with 10μM Doxo, 10μM Acla or 10μM Etop for 2 hours. The experiment was performed with biological replicates. Upon treatment cells were fixed and processed as describes [36]. For immunoprecipitation mouse anti-IFI16 (Santa Cruz, sc-8023) was used. DNA was processed to be sequenced following a standard TrueSeq library preparation for the Illumina HiSeq2000 platform. All samples were quality controlled and processed in the same way before further analyzed. ChIP peak calling was measured by a binarized genome with a 500 bp window. Differential expressed peaks were determined using MACS version 2.1.1.20160309 software.

Bio-ID and Mass spectrometry
For Bio-ID, HEK293T cells were seeded in a 10cm dish, transfected 16 hours later with the BirA-GFP constructs using PEI-transfection reagent. Cell were incubated with 50 μM biotin for 3 hours and lysed for 30 minutes in lysis buffer (50mM Tris-HCl pH 8.0, 150mM Nacl, 5mM $MgCl_2$, 0.5% NP-40 supplemented with protease inhibitors (Roche 7 Diagnostics, EDTA free). Supernatant after spinning (15min. at 12000g) was incubated with High Capacity Neutravidin Agarose Resin beads (Thermo Scientific) for 1 hour. Beads were extensively washed in washing buffer (50mM Tris-HCl pH 8.0, 150mM NaCl, 5mM $MgCl_2$, 0.08% NP-40 supplemented with 1% SDS) before addition of Laemmli Sample Buffer (containing 5% β-mercaptoethanol) followed by 10 minutes incubation at 95°C. Immunoprecipitated proteins were separated by SDS-PAGE, lanes were cut from the silver stained (Invitrogen) gel and subjected to reduction by dithiothreitol, alkylation with iodoacetamide and in-gel trypsin digestion using a Proteineer DP digestion robot (Bruker). Tryptic peptides were extracted from the gel, lyophilized, dissolved in 95/3/0.1 v/v/v water/acetonitril/formic acid and subsequently analyzed by on-line nanoHPLC MS/MS using an 1100 HPLC system (Agilent Technologies), as previously described [37]. Peptides were trapped at 10 μl/min on a 15-mm column (100-μm ID; ReproSil-Pur C18-AQ, 3 μm, Dr. Maisch GmbH) and eluted to a 200 mm column (50-μm ID; ReproSil-Pur C18-AQ, 3 μm) at 150 nl/min. All columns were packed in house. The column was developed with a 30-min gradient from 0 to 50% acetonitrile in 0.1% formic acid. The end of the nanoLC column was drawn to a tip (5-μm ID), from which the eluent was sprayed into a 7-tesla LTQ-FT Ultra mass spectrometer (Thermo Electron). The mass spectrometer was operated in data-dependent mode, automatically switching between MS and MS/MS acquisition. Full scan MS spectra were acquired in the FT-ICR with a resolution of 25,000 at a target value of 3,000,000. The two most intense ions were then isolated

for accurate mass measurements by a selected ion-monitoring scan in FT-ICR with a resolution of 50,000 at a target accumulation value of 50,000. Selected ions were fragmented in the linear ion trap using collision-induced dissociation at a target value of 10,000. In a post-analysis process, raw data were first converted to peak lists using Bioworks Browser software v3.2 (Thermo Electron), and then submitted to the Swissprot database version 51.6 (257,964 entries), using Mascot v. 2.2.04 (www.matrixscience.com) for protein identification. Mascot searches were with 2 ppm and 0.8 Da deviation for precursor and fragment mass, respectively, and trypsin as enzyme. Protein was finally sorted and compared using Scaffold software version 3.0.1 (www. proteomesoftware.com).

Co-immunoprecipitation
For co-immunoprecipitation experiments, HEK293T cells were seeded, transfected 16 hours later using PEI-transfection reagent and lysed for 30 minutes at 4°C in lysis buffer (50mM Tris-HCl pH 8.0, 150mM NaCl, 5mM $MgCl_2$, 0.5% NP-40 supplemented with protease inhibitors (Roche 7 Diagnostics, EDTA free). Supernatant after spinning (15min at 12000g) was incubated with GFP-trap agarose beads (ChromoTek) for 1 hour. Beads were washed four times in wash buffer (50mM Tris-HCl pH 8.0, 150mM NaCl, 5mM $MgCl_2$, 0.08% NP-40) before addition of Laemmli Sample buffer (containing 5% β-mercaptoethanol) followed by 10 minutes incubation at 95°C. Co-immunoprecipitated proteins were separated by SDS-PAGE for Western blotting and detection by antibody staining. Antibody signals were detected by Chemidoc XRS+ imager (Bio-Rad).

Ubiquitination assay
HEK293T cells were lysed for 30 min in lysis buffer (50mM Tris-HCl pH7.5, 150mM NaCl, 5mM $MgCl_2$, 5mM EDTA, 0.5%TX100, 0.2% SDS, freshly added 10mM NMM (DUB inhibitor diluted in DMSO) and protease inhibitors (Roche Diagnostics, EDTA free). Supernatants were sonicated (Branson Sonifier 250, 3 pulses, 70%) followed by spinning (15 min at 12,000g), and incubated with incubated with GFP-trap agarose beads (ChromoTek) for 1 hour. Beads were washed four times in lysis buffer before addition of Laemmli Sample Buffer (containing 5% β-mercaptoethanol) followed by 10 min incubation at 95°C. Proteins were separated by SDS-PAGE, transferred to nitrocellulose membranes and detected by antibodies. Li-Cor fluorescent dyes were used as secondary antibodies and detected by an Odyssey Classic imager (Li-Cor).

Western blotting
SDS-sample buffer (2% SDS, 10% glycerol, 5% β-mercaptoethanol, 60mM Tris-HCl pH 6.8 and 0.01% bromophenol blue) was added to the samples. Samples were separated by a 10% acrylamide gel followed by western blotting. Primary antibodies used for blotting: anti-GFP (generated in house, NKI, The Netherlands, 1:1000 [31]), HRP-conjugated anti-FLAG M2 (Mouse, A8592, Sigma, 1:5000), mouse anti-FLAG M2 (F3165, Sigma, 1:5000), mouse anti-HA (16B12, Covance, 1:1000), mouse anti-β-actin (A5441, Sigma, 1:10000), mouse anti-β-actin (A5441, Sigma, 1:10000), mouse anti-IFI16 (Santa Cruz, sc-8023, 1:500). Images were quantified using ImageJ software.

***In vitro* cell viability assay**
MelJuSo cells were seeded into 96-well plates in the presence or absence of IFNβ or IFNγ (100ng/ml). Twenty-four hours after seeding, cells were treated with indicated

drugs for 2 hours at various concentrations. Subsequently, drugs were removed and cells were left to grow for an additional 72 hours. Cell viability was measured using the CellTiter-Blue viability assay (Promega). Relative survival was normalized to the untreated control and corrected for background signal

REFERENCE

1. Weiss, R. B. (1992) The Anthracyclines - Will We Ever Find a Better Doxorubicin, Semin Oncol. 19, 670-686.
2. Hortobagyi, G. N. (1997) Anthracyclines in the treatment of cancer - An overview, Drugs. 54, 1-7.
3. Pommier, Y. (1993) DNA Topoisomerase-I and Topoisomerase-Ii in Cancer-Chemotherapy - Update and Perspectives, Cancer Chemoth Pharm. 32, 103-108.
4. Nitiss, J. L. (2009) Targeting DNA topoisomerase II in cancer chemotherapy, Nat Rev Cancer. 9, 338-350.
5. Pang, B. X., Qiao, X. H., Janssen, L., Velds, A., Groothuis, T., Kerkhoven, R., Nieuwland, M., Ovaa, H., Rottenberg, S., van Tellingen, O., Janssen, J., Huijgens, P., Zwart, W. & Neefjes, J. (2013) Drug-induced histone eviction from open chromatin contributes to the chemotherapeutic effects of doxorubicin, Nat Commun. 4.
6. Yang, F., Kemp, C. J. & Henikoff, S. (2013) Doxorubicin Enhances Nucleosome Turnover around Promoters, Curr Biol. 23, 782-787.
7. McGinty, R. K. & Tan, S. (2015) Nucleosome Structure and Function, Chem Rev. 115, 2255-2273.
8. Ludlow, L. E. A., Johnstone, R. W. & Clarke, C. J. P. (2005) The HIN-200 family: More than interferon-inducible genes?, Exp Cell Res. 308, 1-17.
9. Park, H. H., Lo, Y. C., Lin, S. C., Wang, L., Yang, J. K. & Wu, H. (2007) The death domain superfamily in intracellular signaling of apoptosis and inflammation, Annu Rev Immunol. 25, 561-586.
10. Monroe, K. M., Yang, Z. Y., Johnson, J. R., Geng, X., Doitsh, G., Krogan, N. J. & Greene, W. C. (2014) IFI16 DNA Sensor Is Required for Death of Lymphoid CD4 T Cells Abortively Infected with HIV, Science. 343, 428-432.
11. Kerur, N., Veettil, M. V., Sharma-Walia, N., Bottero, V., Sadagopan, S., Otageri, P. & Chandran, B. (2011) IFI16 Acts as a Nuclear Pathogen Sensor to Induce the Inflammasome in Response to Kaposi Sarcoma-Associated Herpesvirus Infection, Cell Host Microbe. 9, 363-375.
12. Dell'Oste, V., Gatti, D., Gugliesi, F., De Andrea, M., Bawadekar, M., Lo Cigno, I., Biolatti, M., Vallino, M., Marschall, M., Gariglio, M. & Landolfo, S. (2014) Innate Nuclear Sensor IFI16 Translocates into the Cytoplasm during the Early Stage of In Vitro Human Cytomegalovirus Infection and Is Entrapped in the Egressing Virions during the Late Stage, J Virol. 88, 6970-6982.
13. Johnson, K. E., Bottero, V., Flaherty, S., Dutta, S., Singh, V. V. & Chandran, B. (2014) IFI16 Restricts HSV-1 Replication by Accumulating on the HSV-1 Genome, Repressing HSV-1 Gene Expression, and Directly or Indirectly Modulating Histone Modifications, Plos Pathog. 10.
14. Ran, Y., Zhang, J., Liu, L. L., Pan, Z. Y., Nie, Y., Zhang, H. Y. & Wang, Y. Y. (2016) Autoubiquitination of TRIM26 links TBK1 to NEMO in RLR-mediated innate antiviral immune response, J Mol Cell Biol. 8, 31-43.
15. Gariglio, M., Azzimonti, B., Pagano, M., Palestro, G., De Andrea, M., Valente, G., Voglino, G., Navino, L. & Landolfo, S. (2002) Immunohistochemical expression analysis of the human interferon-inducible gene IFI16, a member of the HIN200 fam-

ily, not restricted to hematopoietic cells, J Interf Cytok Res. 22, 815-821.
16. W. Wei, C. J. C., G. R. Somers, K. S. Cresswell, K. A. Loveland, J. A. Trapani & R. W. Johnstone. (2003) Expression of IFI16 in epithelial cellos and lymphoid tissues. , Histochem Cell Biol. 119, 45-54.
17. Choubey, D., Deka, R. & Ho, S. M. (2008) Interferon-inducible IFI16 protein in human cancers and autoimmune diseases, Front Biosci. 13, 598-608.
18. Landolfo, S., Gariglio, M., Gribaudo, G. & Lembo, D. (1998) The Ifi 200 genes: An emerging family of IFN-inducible genes, Biochimie. 80, 721-728.
19. Doroshow, J. H. & Davies, K. J. A. (1986) Redox Cycling of Anthracyclines by Cardiac Mitochondria .2. Formation of Superoxide Anion, Hydrogen-Peroxide, and Hydroxyl Radical, J Biol Chem. 261, 3068-3074.
20. Qiao, X., van der Zanden, S. Y., Wander, D. P. A., Borras, D. M., Song, J. Y., Li, X., van Duikeren, S., van Gils, N., Rutten, A., van Herwaarden, T., van Tellingen, O., Giacomelli, E., Bellin, M., Orlova, V., Tertoolen, L. G. J., Gerhardt, S., Akkermans, J. J., Bakker, J. M., Zuur, C. L., Pang, B., Smits, A. M., Mummery, C. L., Smit, L., Arens, R., Li, J., Overkleeft, H. S. & Neefjes, J. (2020) Uncoupling DNA damage from chromatin damage to detoxify doxorubicin, Proc Natl Acad Sci U S A.
21. Unterholzner, L., Keating, S. E., Baran, M., Horan, K. A., Jensen, S. B., Sharma, S., Sirois, C. M., Jin, T. C., Latz, E., Xiao, T. S., Fitzgerald, K. A., Paludan, S. R. & Bowie, A. G. (2010) IFI16 is an innate immune sensor for intracellular DNA, Nat Immunol. 11, 997-U42.
22. Johnstone, R. W., Kerry, J. A. & Trapani, J. A. (1998) The human interferon-inducible protein, IFI 16, is a repressor of transcription, J Biol Chem. 273, 17172-17177.
23. Gariano, G. R., Dell'Oste, V., Bronzini, M., Gatti, D., Luganini, A., De Andrea, M., Gribaudo, G., Gariglio, M. & Landolfo, S. (2012) The Intracellular DNA Sensor IFI16 Gene Acts as Restriction Factor for Human Cytomegalovirus Replication, Plos Pathog. 8.
24. Johnson, K. E., Bottero, V., Flaherty, S., Dutta, S., Singh, V. V. & Chandran, B. (2014) IFI16 restricts HSV-1 replication by accumulating on the hsv-1 genome, repressing HSV-1 gene expression, and directly or indirectly modulating histone modifications, Plos Pathog. 10, e1004503.
25. Orzalli, M. H., Conwell, S. E., Berrios, C., DeCaprio, J. A. & Knipe, D. M. (2013) Nuclear interferon-inducible protein 16 promotes silencing of herpesviral and transfected DNA, Proc Natl Acad Sci U S A. 110, E4492-501.
26. Johnstone, R. W., Wei, W., Greenway, A. & Trapani, J. A. (2000) Functional interaction between p53 and the interferon-inducible nucleoprotein IFI 16, Oncogene. 19, 6033-6042.
27. Kwak, J. C., Ongusaha, P. P., Ouchi, T. & Lee, S. W. (2003) IFI16 as a negative regulator in the regulation of p53 and p21(Waf1), J Biol Chem. 278, 40899-40904.
28. Sheng, Y., Saridakis, V., Sarkari, F., Duan, S. L., Wu, T. N., Arrowsmith, C. H. & Frappier, L. (2006) Molecular recognition of p53 and MDM2 by USP7/HAUSP, Nat Struct Mol Biol. 13, 285-291.
29. Trapani, J. A., Browne, K. A., Dawson, M. J., Ramsay, R. G., Eddy, R. L., Shows, T. B., White, P. C. & Dupont, B. (1992) A Novel Gene Constitutively Expressed in Human Lymphoid-Cells Is Inducible with Interferon-Gamma in Myeloid Cells, Immunogenetics. 36, 369-376.
30. Fujiuchi, N., Aglipay, J. A., Ohtsuka, T., Maehara, N., Sahin, F., Su, G. H., Lee, S. W. & Ouchi, T. (2004) Requirement of IFI16 for the maximal activation of p53 induced by ionizing radiation, J Biol Chem. 279, 20339-20344.

31. van der Kant, R., Fish, A., Janssen, L., Janssen, H., Krom, S., Ho, N., Brummelkamp, T., Carette, J., Rocha, N. & Neefjes, J. (2013) Late endosomal transport and tethering are coupled processes controlled by RILP and the cholesterol sensor ORP1L, J Cell Sci. 126, 3462-3474.
32. Garcia-Nafria, J., Watson, J. F. & Greger, I. H. (2016) IVA cloning: A single-tube universal cloning system exploiting bacterial In Vivo Assembly, Sci Rep-Uk. 6.
33. Edmonds, M. J., Carter, R. J., Nickson, C. M., Williams, S. C. & Parsons, J. L. (2017) Ubiquitylation-dependent regulation of NEIL1 by Mule and TRIM26 is required for the cellular DNA damage response, Nucleic Acids Res. 45, 726-738.
34. Sapmaz, A., Berlin, I., Bos, E., Wijdeven, R. H., Janssen, H., Konietzny, R., Akkermans, J. J., Erson-Bensan, A. E., Koning, R. I., Kessler, B. M., Neefjes, J. & Ovaa, H. (2019) USP32 regulates late endosomal transport and recycling through deubiquitylation of Rab7, Nat Commun. 10.
35. Jongsma, M. L. M., Berlin, I., Wijdeven, R. H. M., Janssen, L., Janssen, G. M. C., Garstka, M. A., Janssen, H., Mensink, M., van Veelen, P. A., Spaapen, R. M. & Neefjes, J. (2016) An ER-Associated Pathway Defines Endosomal Architecture for Controlled Cargo Transport, Cell. 166, 152-166.
36. Schmidt, D., Wilson, M. D., Spyrou, C., Brown, G. D., Hadfield, J. & Odom, D. T. (2009) ChIP-seq: Using high-throughput sequencing to discover protein-DNA interactions, Methods. 48, 240-248.
37. Meiring, H. D., van der Heeft, E., ten Hove, G. J. & de Jong, A. P. J. M. (2002) Nanoscale LC-MS(n): technical design and applications to peptide and protein analysis, J Sep Sci. 25, 557-568.

SUPPLEMENTAL INFORMATION

7

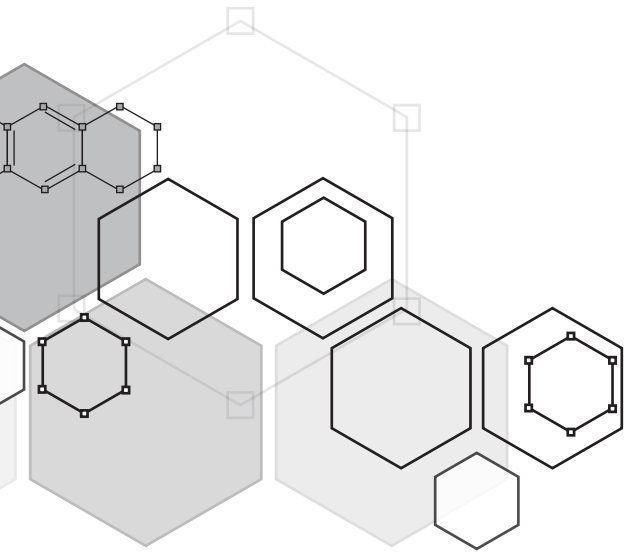

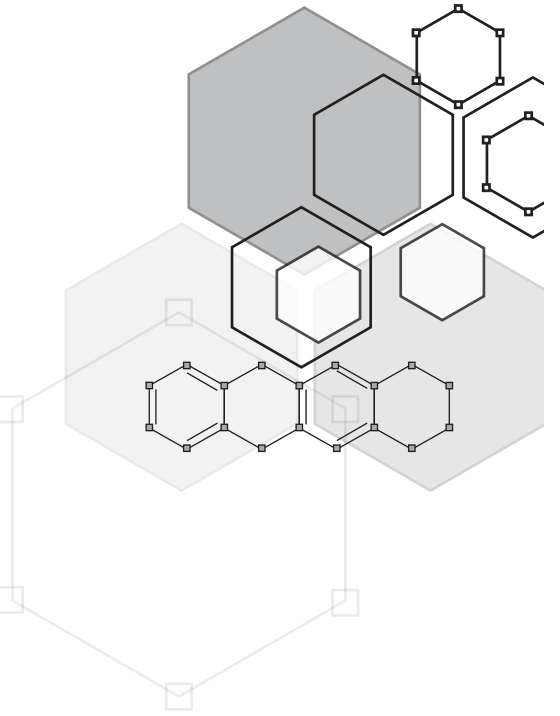

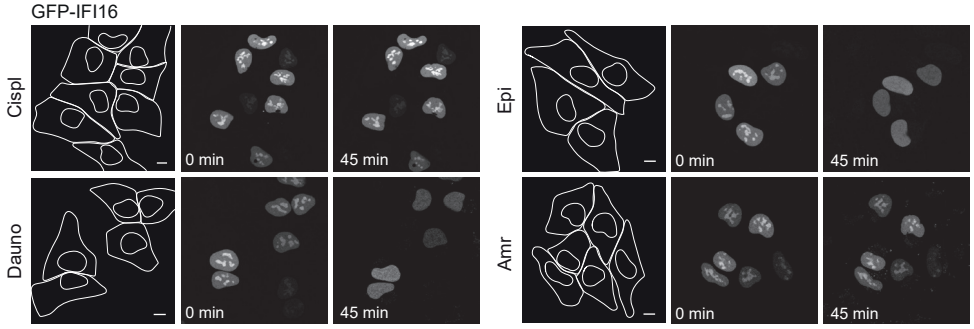

Figure S1. Nuclear DNA sensor IFI16 re-localize upon histone eviction. *MelJuSo cells transiently expressing GFP-tagged IFI16 are followed over time upon treatment with various drugs: Cispl 10μM, Dauno 5μM, Epi 10 μM or Amr 10 μM. Scale bar, 10 μm.*

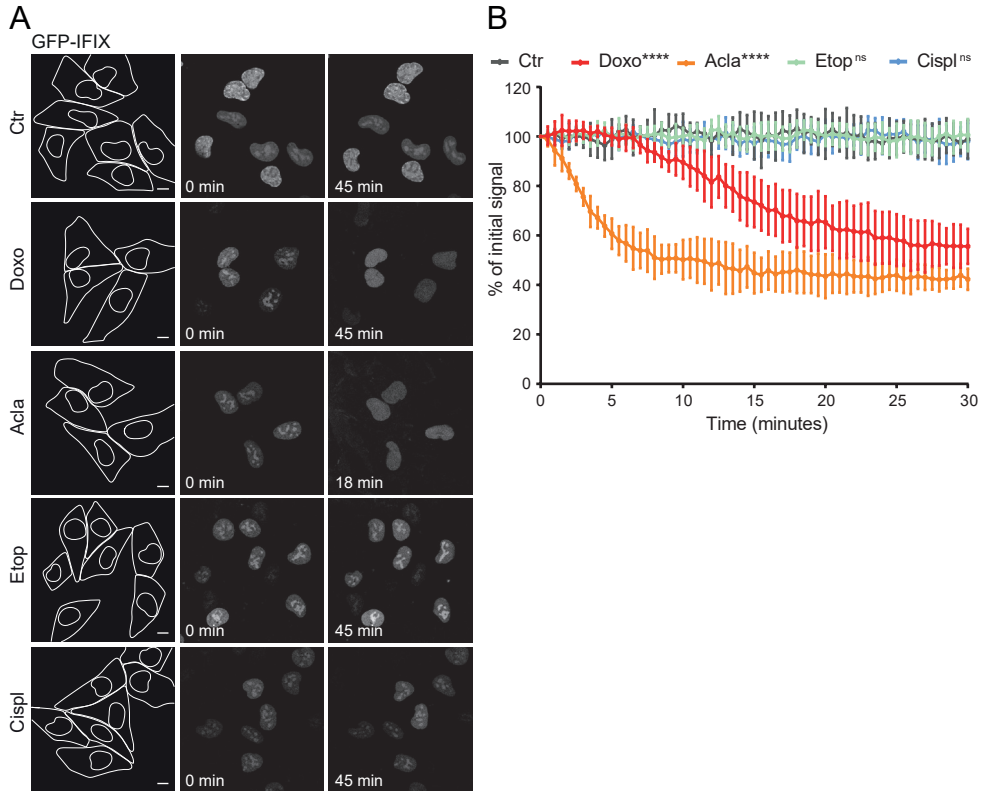

Figure S2. Nuclear DNA sensor IFIX re-localize upon histone eviction. *(A) MelJuSo cells transiently expressing GFP-tagged IFIX are followed over time upon treatment with various drugs: Doxo 10μM, Acla 5μM, Etop 10μM, Cispl 10μM. Scale bar, 10 μm. (B) Quantification of the fluorescent intensity in the nucleoli of cells in A. Ordinary Two-way ANOVA with Turkey's multiple comparison test; ns, not significant; ****P < 0,0001.*

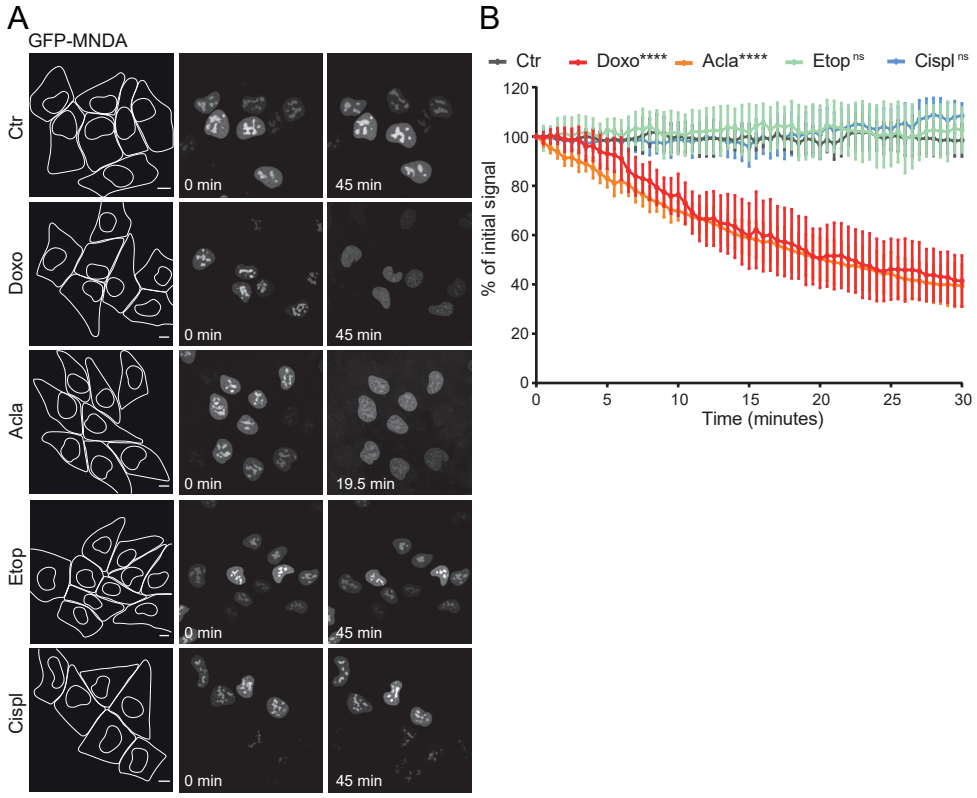

Figure S3. Nuclear DNA sensor MNDA re-localize upon histone eviction. *(A) MelJuSo cells transiently expressing GFP-tagged MNDA are followed over time upon treatment with various drugs: Doxo 10μM, Acla 5μM, Etop 10μM, Cispl 10μM. Scale bar, 10 μm. (B) Quantification of the fluorescent intensity in the nucleoli of cells in C. Ordinary Two-way ANOVA with Turkey's multiple comparison test; ns, not significant; ****P < 0,0001.*

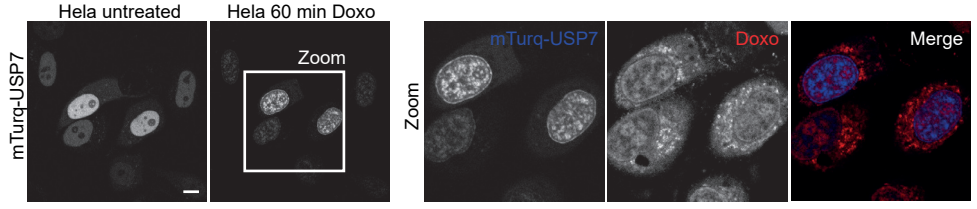

Figure S4. USP7 re-localize upon Doxo treatment. *USP7 localization in Hela cells transiently expressing mTurq-USP7 upon treatment with Doxo 10μM for 1 hour. Scale bar, 10 μm.*